STRUCTURE AND ELECTROPHYSICAL PROPERTIES OF A GaSb–CrSb EUTECTIC COMPOSITE

R. N. Rahimov, I. Kh. Mammadov*, M. V. Kazimov, D. H. Arasly, and A. A. Khalilova

Institute of Physics of the Azerbaijan National Academy of Sciences;
**Azerbaijan National Academy of Aviation*
E-mail: rashadrahim48@gmail.com

(Received June 22, 2015)

Abstract

XRD analysis and microstructure and DSC studies of GaSb-CrSb eutectic composite synthesized by the Bridgman method have been conducted. It has been shown that needle-shaped CrSb inclusions oriented to the solidification direction take part in the GaSb matrix. The initial and final temperature and enthalpy of melting for this composite have been determined. The anisotropy observed in the temperature dependences of Hall coefficient, electrical conductivity, and thermoelectric power of the composite has been attributed to the sort-circuiting effect of metallic inclusions.

1. Introduction

Semimagnetic or diluted magnetic semiconductors are promising materials for the production of high-speed memory systems. It is well known that dilute magnetic semiconductors based on binary semiconductors doped with 3*d*-transition metals do not have stable characteristics. From this point of view, eutectic composites based on III–V compounds and 3d-transition metals (Fe, Mn, Co) have reproducible and stable characteristics and do not depend on external factors [1–4]. These composites are promising targets for researchers because of semiconductor and metal properties. These materials consist of a III–V group semiconductor matrix and metal inclusions parallel oriented in the matrix. In these systems, the charge carriers are redistributed at semiconductor–metal boundaries and structural and electronic energy states arise, the fact that is not characteristic of each phase individually. These semiconductor–metal eutectic composites exhibit a behavior similar to that of nonuniform semiconductors. The physical properties of these materials strongly depend on the electronic configuration of 3*d*-elements, geometry of inclusions, and the formation of interphase zones between the inclusions and the matrix [5–6].

Previously, we investigated the features of the electron–phonon processes of the eutectic composites based on GaSb and InSb compounds with Fe, Co, and Mn [3–6]. The present work is focused on the synthesis, differential scanning calorimeter (DSC) analysis, and studies of the microstructure and electrophysical parameters of a GaSb–CrSb composite in a temperature range of 80–750 K as a continuation of a cycle of works of the preparation and investigation of eutectic composites.

2. Experimental

The synthesis of GaSb–CrSb eutectic composite was conducted in two stages. Semiconductor GaSb was prepared by alloying the related components in stoichiometric quantities and refining the alloy by horizontal recrystallization method. The eutectic alloys of GaSb–CrSb have been prepared by alloying GaSb and 13.5 wt% CrSb using the vertical Bridgman method. The rate of the crystallization front was set at about 0.3 mm/min. The resulting crystals exhibited *p*-type conductivity.

XRD intensity data were collected on an Advance-D8 diffractometer using CuK_α radiation. The microstructure and elemental composition of the samples were studied using a FEI Quanta FEG electron microscope and an Oxford Inca X-act EDS system.

The heat flow (DSC) and mass change (TG) were recorded on a PerkinElmer STA 6000 instrument (United States) in a nitrogen atmosphere with a gas flow rate of 20 mL/min and at a heating rate of 10°C/min. The sample with a weight of 123.547 mg was placed in a corundum crucible. The DTA curve was derived from DSC curve differentiation.

The electrical properties of the composite were investigated by means of compensation in a temperature range of 80–750 K and at a magnetic field of 1.3 T in the mutual directions of the electric current, crystallization, heat flow, and magnetic field.

3. Results and discussion

Diffraction patterns of eutectic composite GaSb–CrSb are shown in Fig. 1. This figure also shows data on the diffraction patterns for GaSb and CrSb compounds. Analysis of XRD spectra using TOPAZ and EVA applications has confirmed that this system is diphasic: the most intense peaks corresponding to the (111), (200), (220), (311), (222), (400), (331), (420), and (422) Muller index are identical to the GaSb matrix, while the weak peaks found at 2θ = 30°, 44.08°, 52.12°, and 54.13° coincide with the CrSb lines having a hexogonal structure with lattice parameters of a = 4.121, c = 5.467, c/a = 1.327, and the *P63/mmc* space group.

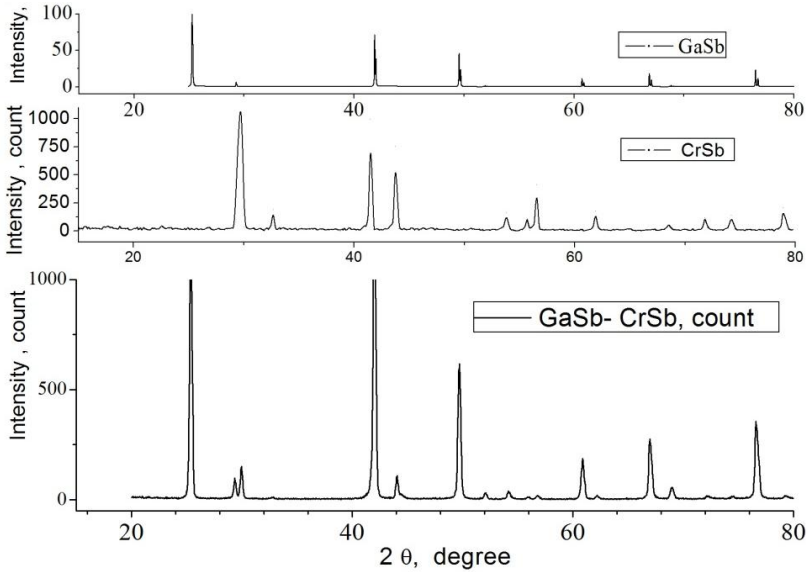

Fig. 1. Comparative diffraction patterns of the GaSb and CrSb compounds and the GaSb–CrSb eutectic composite.

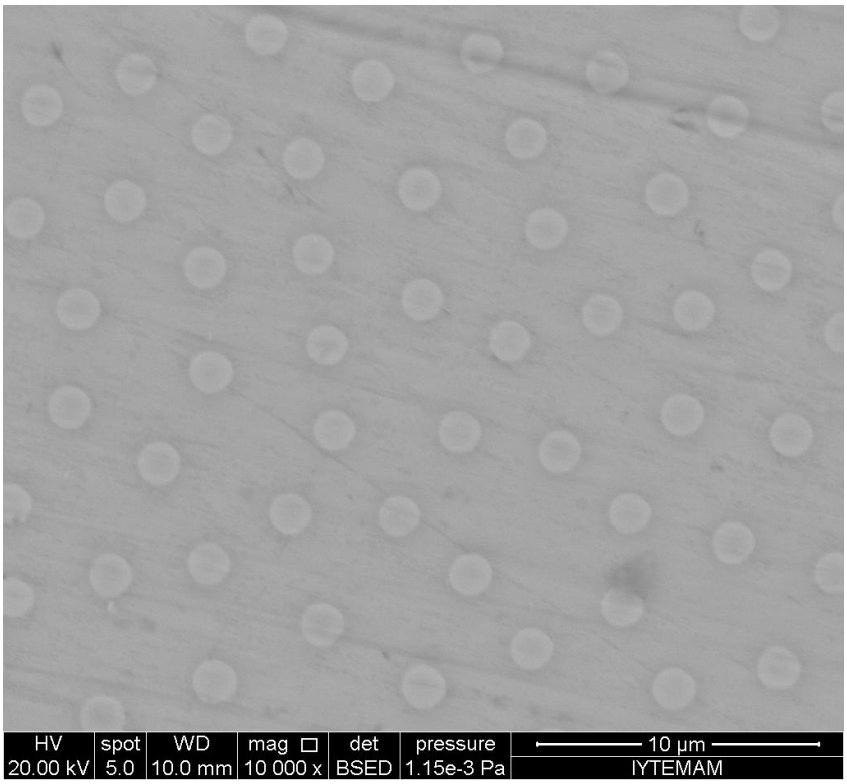

Fig. 2. SEM image of the GaSb–CrSb eutectic composite (magnification of 10000 times).

The data on the microstructure and elemental composition are shown in Figs. 2 and 3. The needle-shaped metallic inclusions are uniformly and parallel distributed in the GaSb matrix. Based on SEM examinations, the oriented needles have a diameter of about 1.4 μm, a length of 20–50 μm, and a density of ~8 x 10^4 mm^{-2}. The elemental composition data correspond to the GaSb matrix and the CrSb inclusions.

DSC, TG, and DTA curves of the composite in a temperature range of 25–1000°C are presented in Fig. 3. It is evident from the TG curve that the change in weight is 0.154%. The temperature range of 670–700°C, in which the endothermic process occurs and the weight remains unchanged, corresponds to the melting of the composite. It has been found that the initial and final melting temperatures are 670 and 692°C, respectively, and the enthalpy of melting is 56.45808 J/g. The temperature range of 645–670°C, in which the endothermic process occurs and the weight increases, corresponds probably to the oxide process with an enthalpy of 6.3335 J/g.

The results of studies of the temperature dependences of the Hall coefficient *R(T)*, electrical conductivity *σ(T*) and thermoelectric power *α(T)* measured at the different mutual directions of current (*I*), magnetic field (*B*), and crystallization direction are shown in Figs. 5–7. In the temperature dependence of the kinetic coefficients, anisotropy due to the presence of regular metal crystalline inclusions in the semiconductor matrix is observed. Due to shorting action by needle-shaped metallic inclusions, the electrical conductivity increases in the $I \parallel x$ direction and it is significantly different from *σ(T)* in the $I \perp x$ direction. The coefficient of conductivity anisotropy at 80 K is $\sigma_{\parallel}/\sigma_{\perp} = 3.2$ and decreases with increasing temperature: $\sigma_{\parallel}/\sigma_{\perp} = 3$ at 300 K. The electrical conductivity decreases in a temperature range of 400–560 K; however,

above 560 K, it greatly increases and anisotropy completely disappears. The decrease in the electrical conductivity is associated with the occurrence of a new flow of conduction electrons compensating for the hole conductivity. The electron contribution to conduction and to the total mobility increases above 560 K. The deviation on the $\sigma(T)$ dependence observed in a temperature range of 600–650K is possible due to the magnetic phase transition of the CrSb inclusions [7, 8].

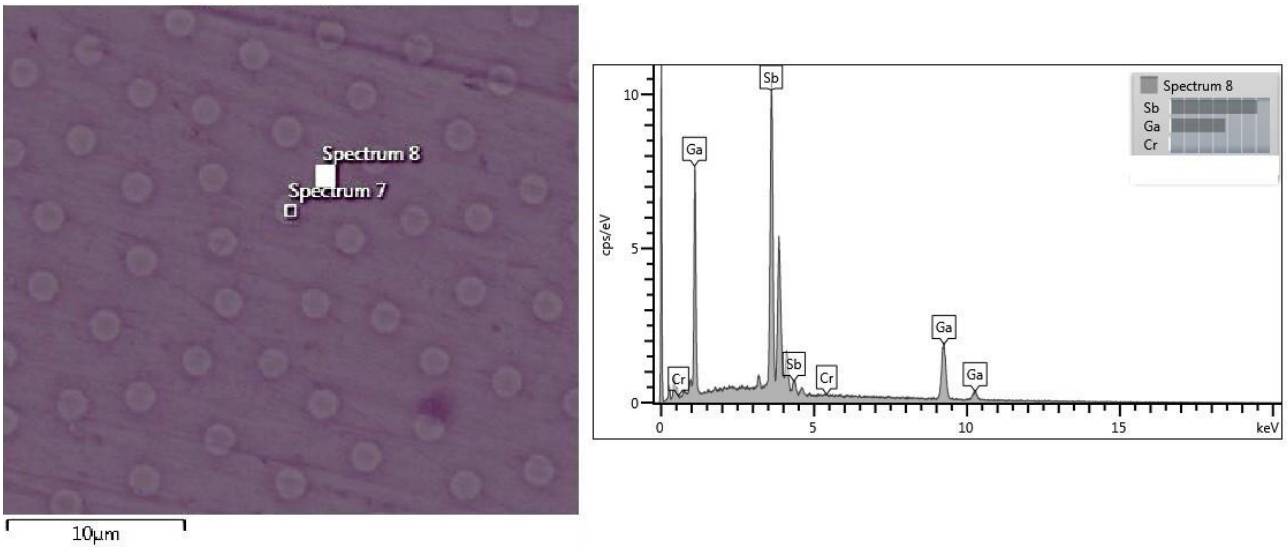

a)

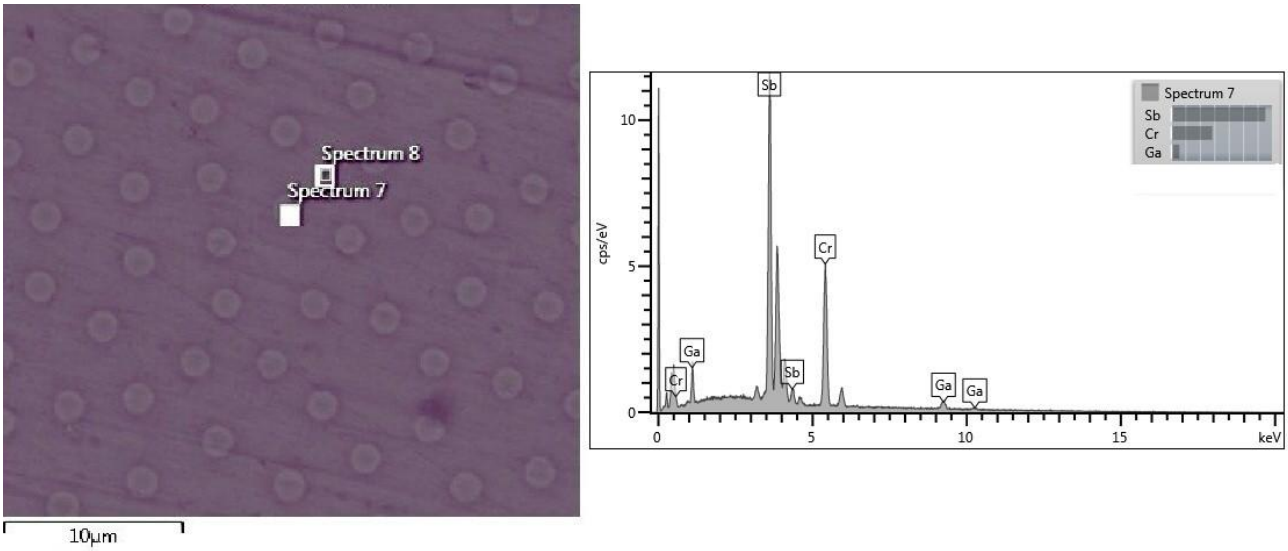

b)

Fig. 3. Elemental compositions of the GaSb–CrSb composite obtained with SEM–EDX from (a) the matrix and (b) inclusion phases.

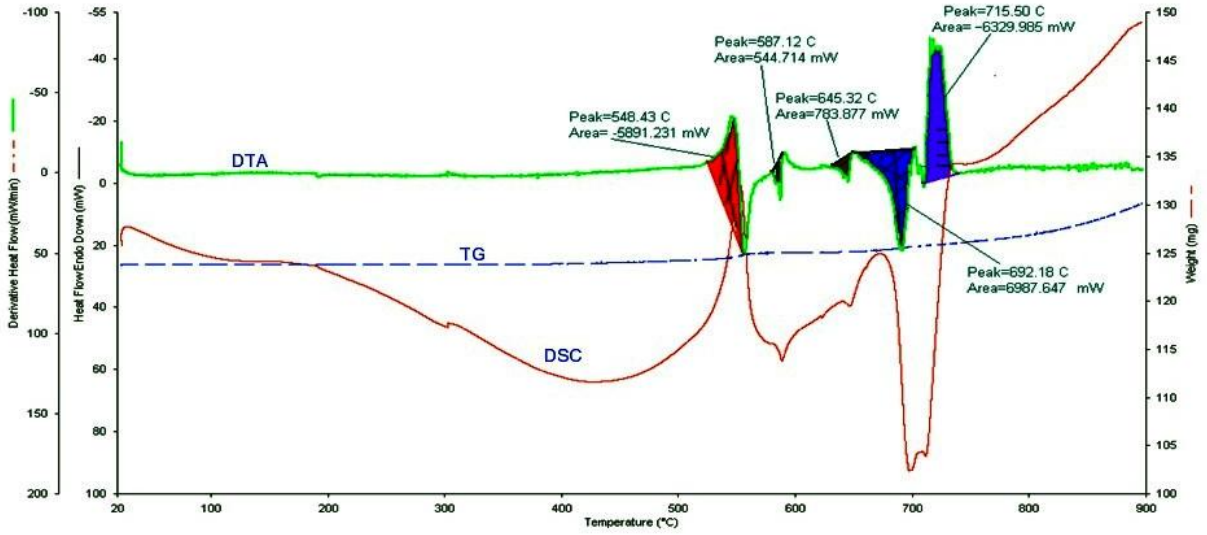

Fig. 4. DSC, TG, and DTA curves of the GaSb–CrSb composite.

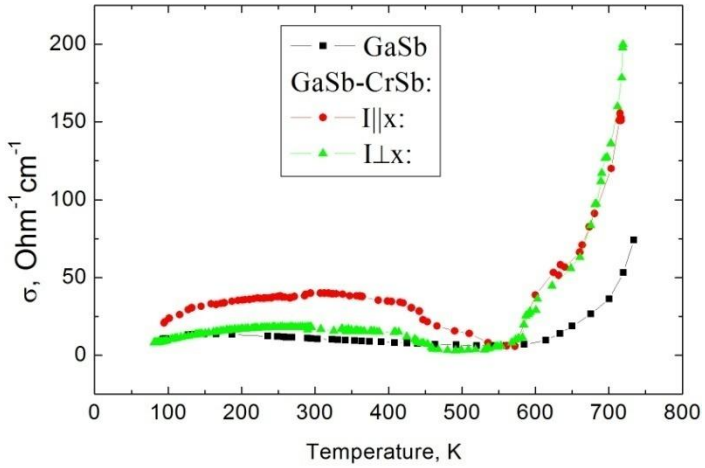

Fig. 5. Temperature dependence of electric conductivity for GaSb and the GaSb–CrSb composite.

As shown in our previous studies [3], the *R* value is maximum if the metallic needles in the matrix are oriented perpendicular to the current direction and parallel to the magnetic field ($I \perp x \parallel B$) and the behavior of the *R(T)* dependence is approximately the same as that for the matrix. The Hall coefficient drop along the sample in the case of $I \parallel x \perp B$ due to the short-circuiting of the voltage and the Hall voltage in the case of $I \perp x \perp B$ has a minimum value. The temperature dependence of the Hall coefficient *R(T)* measured in the case of $I \perp x \parallel B$ where there is no shorting of any current or potential Hall are plotted in Fig. 6. It is evident from the figure that the Hall coefficient remains unchanged in a temperature range of 80–475 K. The sign of the Hall coefficient changes at temperatures between 490 and 515 K (the inversion point for GaSb is ~560 K).

Strong anisotropy is also observed in the temperature dependence of the thermoelectric power (Fig. 7). The short-circuiting of V_α potential by metallic inclusions at $\Delta T \| x$ directions

results from a decrease in the thermopower.

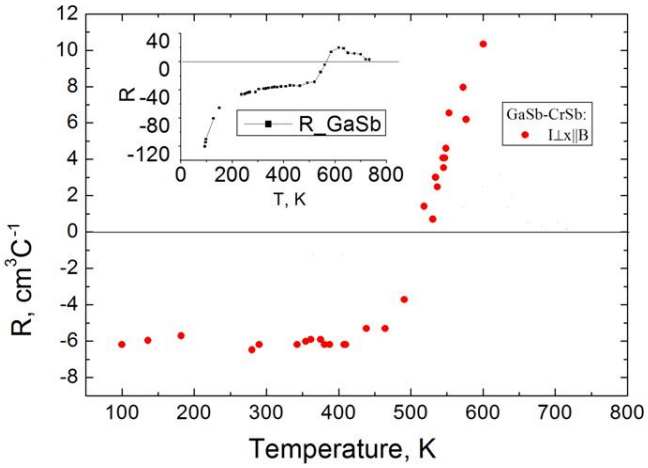

Fig. 6. Temperature dependence of Hall coefficient for GaSb–CrSb composite. The inset shows the (*R(T)* dependence for GaSb.

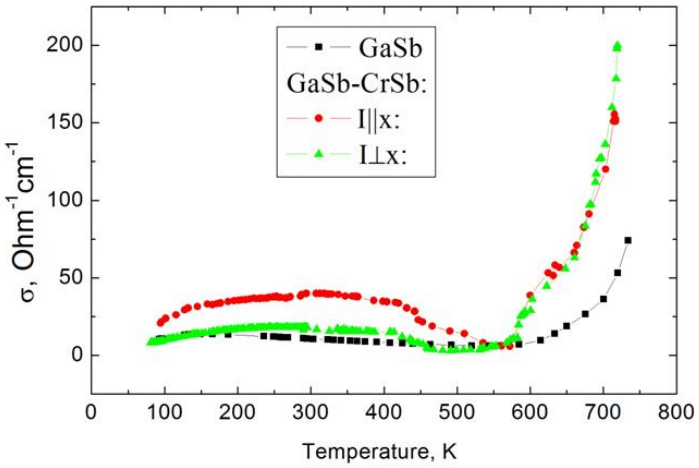

Fig. 7. Temperature dependence of thermoelectric power for the GaSb–CrSb composite.

4. Conclusions

The electron microscopy and XRD studies of GaSb–CrSb have confirmed that the systems consist of a semiconductor matrix and oriented needle-shaped metal inclusions. The initial and final melting temperatures for this composite are 670 and 692°C, respectively; the enthalpy of melting is 56.45808 J/g. The anisotropy observed in the temperature dependence of the kinetic parameters at different mutual directions of current, solidification, magnetic field, and heat flow are attributed to the short-circuiting effect of metallic inclusions. The sign of Hall coefficient of GaSb–CrSb changes in a temperature range between of 490 and 515 K. The deviation in electrical conductivity in a temperature range of 600–650 K is associated with the magnetic phase transition of the CrSb inclusions.

References

[1] A. Müller and M. Wilhem, J. Phys. Chem. Solids, 26, 12, 2029, (1965).
[2] Y. Umehara and S. Koda, J. Jpn. Inst. Met. 50, 7, 666, (1986).
[3] M. I. Aliyev, A. A. Khalilova, D. H. Arasly, R. N. Rahimov, M. Tanoglu, and L. Ozyuzer, J. Phys. D: Appl. Phys. 36, 2627, (2003).
[4] R. N. Rahimov, I. Kh. Mammadov, M. V. Kazimov, D. H. Arasly, and A. A. Xəlilova, J. Qafqaz Univ., Phys. 1, 2, 166, (2013).
[5] M. I. Aliyev, D. H. Arasly, R. N. Rahimov, A. A. Khalilova, I. Kh. Mammadov, and R. M. Jabbarov, Trans. Azerbaijan Nat. Acad. Sci.: Phys. Astron. 27, No. 2, 72, (2007).
[6] M. I. Aliyev, I. Kh. Mammadov, A. A. Khalilova, R. N. Rahimov, and D. H. Arasly, Mold. J. Phys. Sci. 11, No.3, 157, (2012).
[7] T. S. Dijkstra, C. F. Bruggeni, C. Haasi, and R. A. Grooti, J. Phys.: Condens. Matter 1, 9163, (1989).
[8] Yong Liu, S. K. Bose, and J. Kudrnovsky, World J. Eng. **9,** 2, 125, (2012).